

Molecular geometry and electronic structures of stable organic derivatives of divalent germanium and tin $[(\text{Me}_3\text{Si})_2\text{N}-\text{M}-\text{OCH}_2\text{CH}_2\text{NMe}_2]_n$ ($\text{M} = \text{Ge}$, $n = 1$; $\text{M} = \text{Sn}$, $n = 2$): a theoretical study

M. S. Nechaev* and Yu. A. Ustynyuk

Department of Chemistry, M. V. Lomonosov Moscow State University,
1 Leninskie gory, 119992 Moscow, Russian Federation.

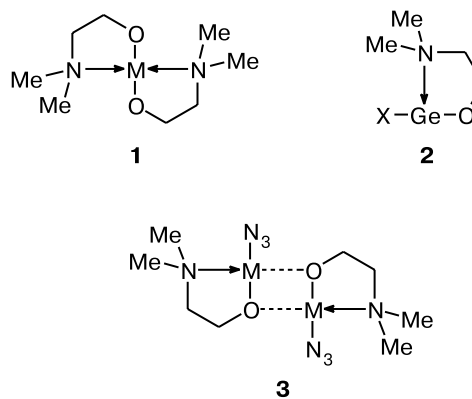
Fax: +7 (095) 939 2677. E-mail: nechaev@nmr.chem.msu.ru

The molecular geometry and electronic structure of stable organic derivatives of divalent germanium and tin, $[(\text{Me}_3\text{Si})_2\text{N}-\text{M}-\text{OCH}_2\text{CH}_2\text{NMe}_2]_n$ ($\text{M} = \text{Ge}$ (**4**), $n = 1$; $\text{M} = \text{Sn}$ (**5**), $n = 2$) and their isomers with broken (**4a**, **5a**) and closed (**4b**, **5b**) intramolecular coordination bonds $\text{M} \leftarrow \text{NMe}_2$, were studied by the density functional (PBE/TZ2P/SBK-JC) and NBO methods. Factors responsible for stability of their dimers **4c** and **5c** were established. Dimerization of **5b** in the gas phase is a thermodynamically favorable process ($\Delta G^0 = -2.1 \text{ kcal mol}^{-1}$) while that of **4b** is thermally forbidden ($\Delta G^0 = 10.1 \text{ kcal mol}^{-1}$), which is consistent with experimental data. The $\text{M} \leftarrow \text{NMe}_2$ coordination bond energies, ΔE^0 , were found to be -5.3 and $-8.6 \text{ kcal mol}^{-1}$ for $\text{M} = \text{Ge}$ and Sn , respectively. NBO analysis showed that the metal atoms M in molecules **4** and **5** are weakly hybridized. The lone electron pairs of the M atoms have strong s-character while vacant orbitals of these atoms, $\text{LP}^* \text{M}$, are represented exclusively by the metal np_z -AOs. The strongest orbital interactions between subunits in dimers **4c** and **5c** involve electron density donation from the lone electron pairs of oxygen atoms (LP O) to the $\text{LP}^* \text{M}$ orbitals.

Key words: germylene, stannylene, molecular geometry, electronic structure, quantum-chemical calculations, density functional theory, natural bonding orbitals, X-ray analysis.

Chemistry of organic derivatives of divalent germanium and tin, namely, germylenes and stannylenes and related organic compounds with element–heteroatom covalent bonds has been rapidly developing in the last two decades. Very high reactivities of these heavy carbene analogs and their ability to form coordination polymers is due to the fact that the metal atom has a low-lying lowest unoccupied molecular orbital (LUMO) and the lone electron pair (LEP) that occupies a high-lying highest occupied molecular orbital (HOMO). Some of these compounds can be obtained as relatively stable monomers using steric and electronic stabilization factors. Steric stabilization can be achieved by introducing bulky substituents to the metal atom in order to prevent intermolecular reactions.^{1–4} Electronic stabilization can be attained in three main ways. Introduction of electron-acceptor groups to the metal atom (M) decreases the HOMO energy.⁵ Coordination of donor groups (NR_2 , OR , etc.) to the atom M causes the LUMO to be shielded;⁶ this orbital can also be shielded against external attack by involving in the formation of a stable aromatic system (π -electron sextet).^{7–8} Recently, we have synthesized a number of germanium(II) and tin(II) derivatives without bulky sub-

stituents at the metal atom, namely, $\text{M}(\text{OCH}_2\text{CH}_2\text{NMe}_2)_2$ (**1**) ($\text{M} = \text{Ge}$, Sn),⁹ $\text{X}-\text{Ge}-\text{OCH}_2\text{CH}_2\text{NMe}_2$ (**2**) ($\text{X} = \text{Cl}$, OAc),¹⁰ $[\text{N}_3-\text{M}-\text{OCH}_2\text{CH}_2\text{NMe}_2]_2$ (**3**) ($\text{M} = \text{Ge}$, Sn),¹¹ and $(\text{Me}_3\text{Si})_2\text{N}-\text{Ge}-\text{OCH}_2\text{CH}_2\text{NMe}_2$ (**4**), and $[(\text{Me}_3\text{Si})_2\text{N}-\text{Sn}-\text{OCH}_2\text{CH}_2\text{NMe}_2]_2$ (**5**) (Fig. 1).¹² These compounds are stabilized through electronic factors only, namely, by introducing electron-acceptor atoms O to the



1, 3: $\text{M} = \text{Ge}$, Sn ; **2:** $\text{X} = \text{Cl}$, OAc

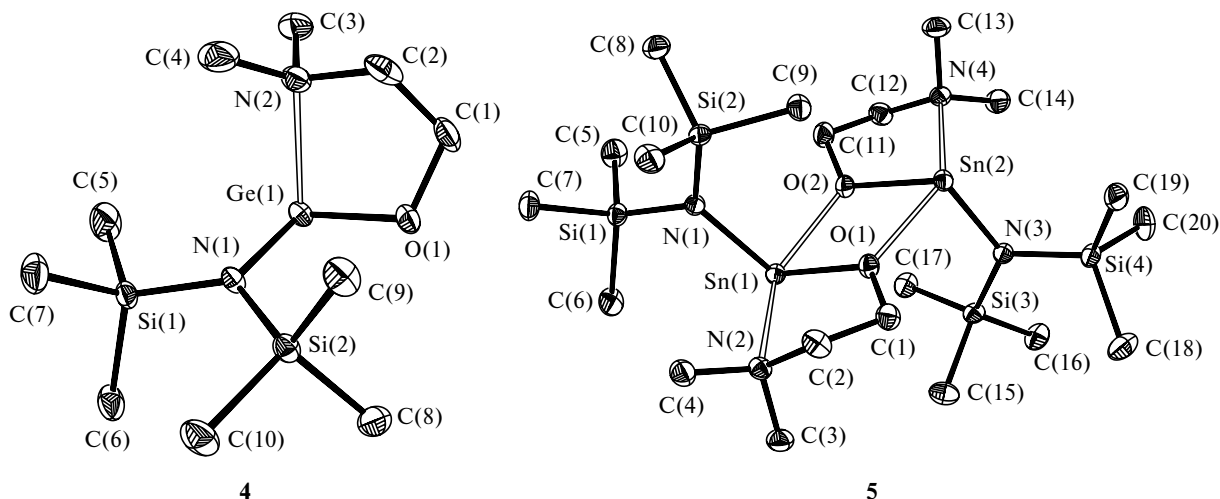


Fig. 1. Crystal structures of compounds $(\text{Me}_3\text{Si})_2\text{N}-\text{Ge}-\text{OCH}_2\text{CH}_2\text{NMe}_2$ (**4**) and $[(\text{Me}_3\text{Si})_2\text{N}-\text{Sn}-\text{OCH}_2\text{CH}_2\text{NMe}_2]_2$ (**5**).¹²

atom M accompanied by coordination of one or two NMe_2 donor groups in the side chain.

The molecular and electronic structure of compounds **1** and **2** were studied by X-ray analysis and using theoretical methods.^{9,10} It was found that the predominant role in their stabilization is played by the formation of coordination bonds $\text{M} \leftarrow \text{NMe}_2$ with energies ranging between 10 and 15 kcal mol⁻¹. In the crystal, compounds **1** and **2** exist as monomers, while molecules of compound **3** form dimers linked by additional intermolecular $\text{M} \leftarrow \text{O}$ coordination bonds. Even more interesting are the structures of two amido derivatives, **4** and **5**, with $(\text{Me}_3\text{Si})_2\text{N}$ groups at the metal atoms. These compounds exist in the crystal as a monomer (**4**) and a coordination dimer (**5**) (see Fig. 1).¹²

In order to gain a better insight into the factors responsible for the existence of these forms of compounds **4** and **5**, in this work we studied these systems using the density functional theory (DFT). We calculated the energies of formation of intramolecular coordination bonds $\text{M} \leftarrow \text{NMe}_2$ and analyzed the types of bonding (i) between the metal atoms and substituents and (ii) between substituents in intermolecular complexes by the NBO method.

Calculation Procedure

The molecular geometries of the compounds under study were optimized by the DFT method with the generalized gradient-corrected functional PBE,¹³ which was earlier tested with various classes of molecules.^{14,15} Calculations were carried out using a triple-zeta basis set augmented with polarization functions (TZ2P) of dimension $\{3,1,1/3,1,1/1,1\}$ for Sn, Ge, C, N, and O atoms and $\{3,1,1/1\}$ for H atom.¹⁶ The atom core electrons were represented by the ECP-SBKJC effective core potentials.^{17–19} All stationary points on the potential energy surfaces (PES) were characterized by calculating the frequencies of normal vibrations. No imaginary frequencies were obtained (this corresponded to minima on the PES) except for the cases where

calculations were performed with the interatomic distances obtained by X-ray analysis. The atomic charges were calculated according to Hirshfeld.²⁰ The molecular geometry, vibrational frequency, and atomic charge calculations were performed using the "Priroda" program.²¹ Earlier,²² we successfully used this approach and program in studies of the structure and reactivity of heteroorganic betaines, compounds with multiple bonds $\text{R}_2\text{M}=\text{X}$, and heavy carbene analogs $:\text{MR}_2$ ($\text{M} = \text{Si}, \text{Ge}, \text{Sn}$; $\text{X} = \text{CR}_2, \text{O}, \text{S}, \text{NR}, \text{Se}$; $\text{R} = \text{Alk}, \text{Ar}$).

The electronic structures of the monomers and dimers of molecules **4** and **5** were studied using the natural bonding orbital (NBO) approach^{23–26} also using the PBE functional, TZ2P basis set, and ECP-SBKJC effective potentials. Calculations were carried out using the NBO 4.M program²⁷ incorporated into the PC GAMESS version* of the GAMESS (US) QC program package.²⁸

In the text below we use the following notations²⁷: BD and BD* are respectively the bonding and antibonding natural orbitals, LP are the lone electron pairs, and LP* are the vacant NBOs. NBO hybridizations are given with allowance for normalization of the s-orbital contribution to unity. The notation "sp^x hybridization" means that in the linear expansion the s-orbital coefficient is $1/(1+x)$ and the p-orbital coefficient is $x/(1+x)$. For instance, for the sp⁹ hybridization one gets the coefficients 1/10 for the s-orbital and 9/10 for the p-orbitals.

In this work we studied compounds **4a** and **5a** (isomers of compounds **4** and **5** with broken coordination bonds $\text{M} \leftarrow \text{NMe}_2$), **4b** and **5b** (monomers with coordination bonds $\text{M} \leftarrow \text{NMe}_2$), and dimers **4c** and **5c** (Fig. 2).

Results and Discussion

The calculated geometric parameters of the structures of monomer **4b** and dimer **5c** are in good agreement with the results obtained by X-ray analysis. Differences are at most 0.05 Å for the valence bond lengths and 5° for the

* A. A. Granovskii, <http://classic.chem.msu.su/gran/game/ss/index.html>.

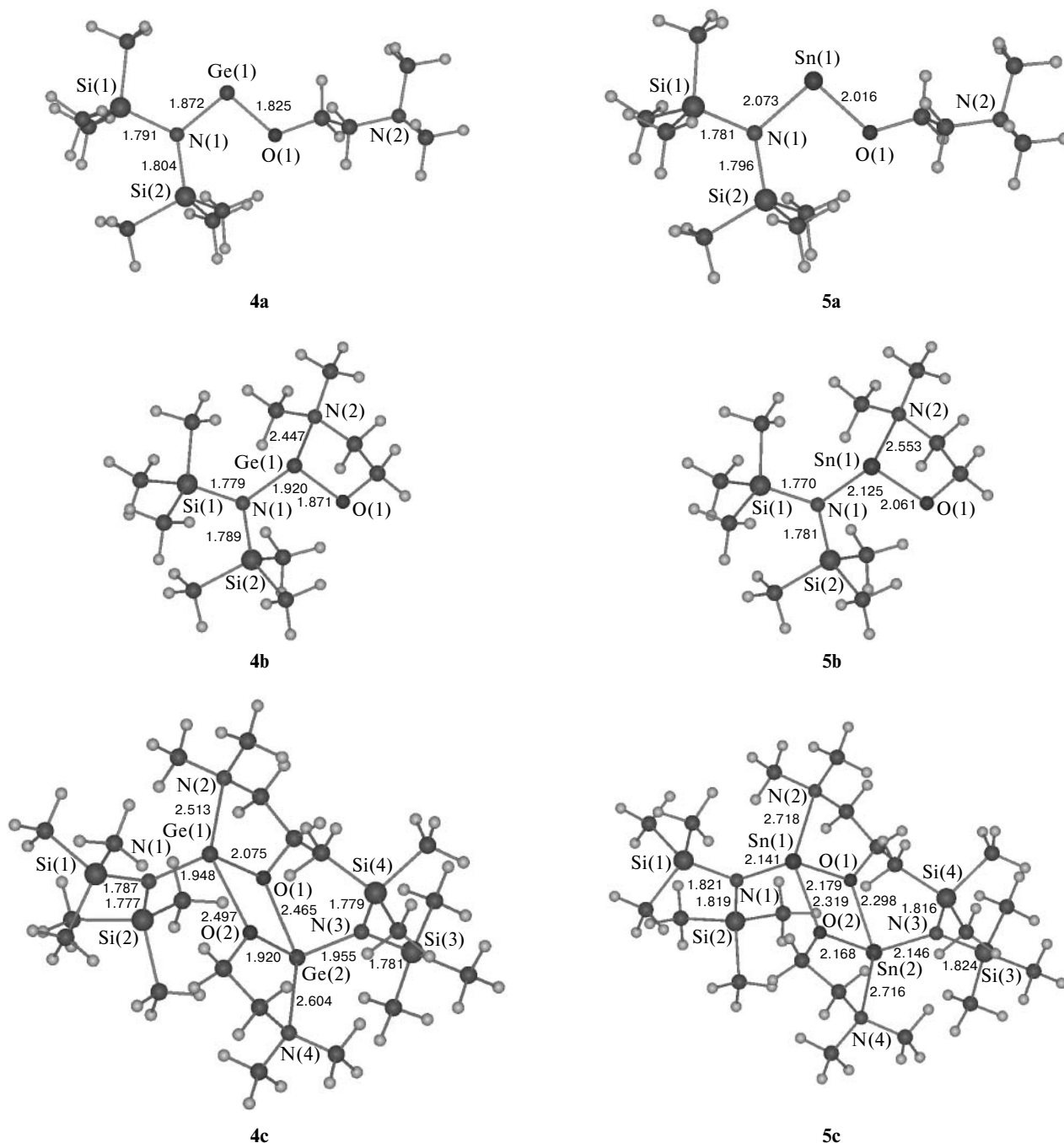


Fig. 2. Calculated molecular structures of **4a–c** and **5a–c** (bond lengths are given in Å).

bond angles (Tables 1 and 2). These discrepancies between the calculated and experimental values are typical of the computational method employed.^{14,15}

The $M \leftarrow NMe_2$ ($M = Ge, Sn$) coordination bond lengths differ much larger. Calculations overestimate them by 0.195 Å for the germanium compound **4b** and by 0.101 Å for the tin compound **5c**. We optimized the structures of the monomer **4d** and dimer **5d** in which the lengths of the $M–O$ and $M–N$ valence bonds and the $M \leftarrow NMe_2$

and $M \leftarrow O$ coordination bonds were taken to be equal to the values obtained for compounds **4** and **5** by X-ray analysis. The energy differences were found to be rather small, namely, $E(\mathbf{4d}) - E(\mathbf{4b}) = 1.3$ and $E(\mathbf{5d}) - E(\mathbf{5c}) = 6.6$ kcal mol^{−1} (Table 3). This means that the PES of molecules **4** and **5** in the vicinity of corresponding local minima are so flattened that significant changes in the interatomic distances cause only minor variations of energy. We believe that the differences between the calcu-

Table 1. Selected geometric parameters of molecule **4** (obtained in X-ray study¹²) and calculated by the PBE/TZ2P method for molecules **4a–d** (bond lengths (*d*), bond angles (ω); differences between the calculated and experimental data are given in parentheses)

Parameter	4	4a	4b	4c	4d
Bond			<i>d</i> /Å		
Ge(1)—O(1)	1.850	1.825	1.871 (0.021)	2.075	1.850*
Ge(2)—O(2)	—	—	—	1.931	—
Ge(1)—N(1)	1.909	1.872	1.920 (0.011)	1.948	1.908*
Ge(2)—N(3)	—	—	—	1.955	—
Ge(1)←N(2)	2.253	—	2.447 (0.194)	2.513	2.252*
Ge(2)←N(4)	—	—	—	2.604	—
Ge(1)←O(2)	—	—	—	2.497	—
Ge(2)←O(1)	—	—	—	2.465	—
Angle			ω /deg		
O(1)—Ge(1)—N(1)	97.73	98.4	97.4 (0.3)	100.8	97.4 (0.3)
O(2)—Ge(2)—N(3)	—	—	—	102.1	—
O(1)—Ge(1)←N(2)	82.81	—	79.8 (3.0)	76.1	82.9 (0.1)
O(2)—Ge(2)←N(4)	—	—	—	76.7	—
N(1)—Ge(1)←N(2)	100.68	—	103.8 (3.1)	100.6	101.7 (1.0)
N(3)—Ge(2)←N(4)	—	—	—	97.2	—
Si(1)—N(1)—Ge(1)	114.53	113.9	113.5 (1.0)	111.8	113.6 (0.9)
Si(3)—N(3)—Ge(2)	—	—	—	111.1	—
Si(2)—N(1)—Ge(1)	120.18	122.4	121.6 (1.4)	128.6	121.4 (1.2)
Si(4)—N(3)—Ge(2)	—	—	—	130.7	—

* The parameter value used in geometry optimization was taken to be equal to that obtained in the X-ray study.

lated and experimental (determined by X-ray analysis) geometric parameters are mainly due to the crystal packing effects that were ignored in the calculations of isolated molecules. Earlier,^{9,10} similar (in magnitude) differences between the calculated and experimental values of structural parameters of the germanium(II) and tin(II) compounds with M←NMe₂ coordination bonds were reported for **1** and **2**.

In molecules **4a** and **5a**, the metal atoms are covalently bound to the atoms N(1) and O(1) (atomic numbering scheme is given in Fig. 2) and the coordination bonds with NMe₂ groups are broken (see Fig. 2). In both molecules the N(1) atoms have planar configurations (the sums of the bond angles at the N(1) atoms equal 360°), which is most probably due to bulkiness of the SiMe₃ groups that repel one another, thus precluding pyramidalization of the N(1) atoms. Planar configuration of the N(1) atoms is also favored by the interaction between the nitrogen LEP and the Ge and Sn *p_z*-orbitals.

Table 2. Selected geometric parameters of molecule **5** (obtained in X-ray study¹²) and calculated by the PBE/TZ2P method for molecules **5a–d** (bond lengths (*d*), bond angles (ω); differences between the calculated and experimental data are given in parentheses)

Parameter	5	5a	5b	5c	5d
Bond			<i>d</i> /Å		
Sn(1)—O(1)	2.133	2.016	2.061 (0.046)	2.179	2.133*
Sn(1)—N(1)	2.147	2.073	2.125 (0.006)	2.141	2.147*
Sn(1)←O(2)	2.267	—	—	2.319 (0.052)	2.267*
Sn(1)←N(2)	2.617	—	2.533 (0.101)	2.718	2.617*
Sn(2)—O(2)	2.137	—	—	2.168 (0.031)	2.137*
Sn(2)—N(3)	2.143	—	—	2.146 (0.003)	2.143*
Sn(2)←O(1)	2.299	—	—	2.298 (0.001)	2.299*
Sn(2)←N(4)	2.615	—	—	2.716 (0.101)	2.615*
Angle			ω /deg		
O(1)—Sn(1)—N(1)	106.34	96.0	96.1 (2.5)	103.8	106.4 (2.5)
O(1)—Sn(1)←O(2)	68.45	—	—	67.9 (0.5)	68.5
N(1)—Sn(1)←O(2)	94.24	—	—	99.1 (4.9)	95.5
O(1)—Sn(1)←N(2)	71.14	—	76.3 (0.1)	71.2	72.0 (0.1)
N(1)—Sn(1)←N(2)	90.42	—	99.7 (3.3)	93.7	91.1 (3.3)
O(2)→Sn(1)←N(2)	138.99	—	—	138.9 (0.1)	140.2
O(2)—Sn(2)—N(3)	103.30	—	—	107.5 (4.2)	102.2
O(2)—Sn(2)←O(1)	67.79	—	—	68.5 (0.7)	67.8
N(3)—Sn(2)←O(1)	95.10	—	—	95.8 (0.7)	59.2
O(2)—Sn(2)←N(4)	71.19	—	—	70.9 (0.3)	72.2
N(3)—Sn(2)←N(4)	93.01	—	—	90.6 (2.4)	93.6
O(1)→Sn(2)←N(4)	138.97	—	—	138.9 (0.1)	139.8
Si(1)—N(1)—Sn(1)	111.21	114.9	114.1 (1.7)	112.9	111.4 (1.7)
Si(2)—N(1)—Sn(1)	129.70	121.8	120.2 (2.5)	127.2	130.7 (2.5)
Si(3)—N(3)—Sn(2)	128.40	—	—	130.3 (1.9)	128.4
Si(4)—N(3)—Sn(2)	112.11	—	—	111.5 (0.6)	112.3

* The parameter value used in geometry optimization was taken to be equal to that obtained in the X-ray study.

Table 3. Calculated energy characteristics (E , $E^0 = E + \text{ZPE}$, G_{298} , H_{298} , and the relative energies ΔE , ΔE^0 , ΔH^0 , ΔG^0) of molecules **4a–d** and **5a–d**

Molecule	$-E$	$-E^0$	G_{298}	H_{298}	ΔE	ΔE^0	ΔH^0	ΔG^0
	a.u							
4a	121.13385	120.77229	244.5	190.2	6.0	5.3	5.8	3.0
4b	121.14341	120.78078	244.7	193.3	0.0	0.0	0.0	0.0
1/2 4c	121.13893	120.77676	244.5	200.5	2.8	2.5	2.6	10.1
4d	121.14140	120.77796	244.9	194.4	1.3	—	—	—
5a	120.70215	120.34153	244.0	188.7	9.3	8.6	9.0	6.3
5b	120.71695	120.35529	244.3	191.7	0.0	0.0	0.0	0.0
1/2 5c	120.72111	120.36015	243.1	201.6	−11.9	−11.7	−13.1	−2.1
1/2 5d	120.72543	120.36278	244.7	200.5	−5.3	—	—	—

Monomers **4b** and **5b** contain tricoordinate metal atoms. They form two valence bonds with the atoms N(1) and O(1) and one M←N(2) coordination bond with the nitrogen atom of the NMe₂ group. Similarly to molecules **4a** and **5a**, here the nitrogen atoms N(1) are planar. Coordination of the NMe₂ group to the metal atom leads to elongation of the M—N(1) and M—O(1) bonds by about 0.05 Å compared to the bonds in isomers **4a** and **5a**. This completes the list of significant changes in the bond lengths and bond angles occurred on going from structures **4a** and **5a** to **4b** and **5b**.

The formation of the M←N(2)Me₂ coordination bonds in molecules **4b** and **5b** is more exothermic for the latter ($\Delta E^0 = -5.3$ and -8.6 kcal mol⁻¹, respectively), which is consistent with greater ability of the tin(II) compounds to coordinate donor ligands compared to the germanium(II) compounds. Earlier,^{9,10} we found a similar ratio of the energies of the NMe₂ group coordination to the Sn^{II} and Ge^{II} atoms in studies of compounds **1** and **2**.

Dimers **4c** and **5c** have tetracoordinate metal atoms. Each atom M forms two valence bonds with the atoms N(1) and O(1), one intramolecular coordination bond with the NMe₂ group, and one intermolecular coordination bond with the oxygen atom of the second subunit. Compared to the structures of monomers **4b** and **5b**, the

M—O covalent bonds in dimers **4c** and **5c** are 0.2 Å (M = Ge) and 0.12 Å (M = Sn) longer. Two subunits in dimers **4c** and **5c** form four-membered rings M₂O₂. It should be noted that the Ge←O coordination bonds in **4c** (2.497 and 2.465 Å) are much longer than the Sn←O coordination bonds in **5c** (2.298 and 2.319 Å), though the covalent radius of germanium atom (1.22 Å) is smaller than that of tin atom (1.41 Å).

The formation of dimer **5c** from **5b** is an exothermic process ($\Delta E^0 = -11.7$ kcal mol⁻¹, see Table 3). The energy of dimer **4c** is higher than that of monomer **4b** ($\Delta E^0 = 2.5$ kcal mol⁻¹). This is consistent with experimental data.

The calculated Hirshfeld atomic charges and dipole moments of molecules **4a–c** and **5a–c** are listed in Table 4. The charge distributions obtained for the germanium and tin compounds are similar.

In all the molecules mentioned above the atoms N(1) and O(1) bear rather large negative charges (−0.32—−0.37 and −0.20—−0.26 a.u., respectively). The atomic charges of nitrogen atoms in the NMe₂ groups are small (−0.03—−0.09 a.u.). The formation of the M←NMe₂ coordination bonds (transitions **4a** → **4b** and **5a** → **5b**) and dimerization (transitions **4b** → **4c** and **5b** → **5c**) do not lead to significant changes in the atomic charges. In the tin compounds the atomic charges of N(1),

Table 4. Hirshfeld atomic charges (q) in and dipole moments (μ) of molecules **4a–c** and **5a–c**

Compound	$q/\text{a.u.}$							μ/D
	Ge(1) [Ge(2)]	Sn(1) [Sn(2)]	N(1) [N(3)]	Si(1) [Si(3)]	Si(2) [Si(4)]	O(1) [O(2)]	N(2) [N(4)]	
4a	+0.29	—	−0.32	+0.38	+0.39	−0.20	−0.08	0.80
4b	+0.26	—	−0.34	+0.37	+0.38	−0.23	−0.03	4.13
4c	+0.31 [+0.29]	—	−0.34 [−0.35]	+0.38 [+0.38]	+0.37 [+0.37]	−0.21 [−0.21]	−0.04 [−0.04]	1.02
5a	—	+0.41	−0.34	+0.38	+0.37	−0.23	−0.09	1.43
5b	—	+0.35	−0.36	+0.37	+0.37	−0.26	−0.03	4.51
5c	—	+0.35 [+0.35]	−0.37 [−0.37]	+0.37 [+0.37]	+0.37 [+0.37]	−0.22 [−0.22]	−0.05 [−0.05]	0.78

O(1), and N(2) are only slightly larger than in the corresponding germanium compounds.

In all cases, metal atoms bear large positive charges, the atomic charges of tin (+0.35—+0.41 a.u.) being much larger than those of germanium (+0.26—+0.31 a.u.) in the corresponding compounds.

The dipole moments of isomers **4a** and **5a** are small (0.80 and 1.43 D, respectively). However, they considerably increase to 4.13 (**4b**) and 4.51 D (**5b**) upon the formation of the M←N(2)Me₂ coordination bonds. Dimerization favors spatial charge compensation and the dipole moments decrease to 1.02 (**4c**) and 0.78 (**5c**) D.

The electronic structures and types of bonding in the molecules **4b** and **5b** and in **4c** and **5c** were studied by the

Table 5. Natural bonding orbitals localized in the vicinity of metal atoms in molecules **4b,c** and **5b,c**

Molecule	Orbital	Population	Atom, polarization degree (%)	Hybridization
4b	BD Ge—O	1.96835	Ge, 11.61 O, 88.39	sp ^{12.51} sp ^{3.35}
	BD Ge—N	1.95855	Ge, 13.52 O, 86.48	sp ^{12.12} sp ^{2.59}
	LP Ge	1.96758	Ge, 100.00	sp ^{0.17}
	LP* Ge	0.26508	Ge, 100.00	p
4c	BD Ge(1)—O(1)	1.95943	Ge, 6.06 O, 93.94	sp ^{24.34} sp ^{3.69}
	BD Ge(1)—N(1)	1.95360	Ge, 7.14 O, 92.86	sp ^{9.64} sp ^{2.10}
	LP Ge(1)	1.93061	Ge, 100.00	sp ^{0.10}
	LP* Ge(1)	0.19358	Ge, 100.00	p
	BD Ge(2)—O(2)	1.96780	Ge, 6.50 O, 93.50	sp ^{18.07} sp ^{2.44}
	BD Ge(2)—N(3)	1.95459	Ge, 8.22 O, 91.78	sp ^{10.40} sp ^{2.03}
	LP Ge(2)	1.92398	Ge, 100.00	sp ^{0.12}
	LP* Ge(2)	0.20461	Ge, 100.00	p
5b	BD Sn—O	1.96196	Sn, 9.70 O, 90.30	sp ^{14.78} sp ^{4.36}
	BD Sn—N	1.95114	Sn, 10.81 O, 89.19	sp ^{11.56} sp ^{2.87}
	LP Sn	1.97098	Sn, 100.00	sp ^{0.16}
	LP* Sn	0.22919	Sn, 100.00	p
5c	BD Sn(1)—O(1)	1.96145	Sn, 3.62 O, 96.38	sp ^{19.46} sp ^{7.08}
	BD Sn(1)—N(1)	1.94974	Sn, 5.73 O, 94.27	sp ^{12.61} sp ^{2.22}
	LP Sn(1)	1.91768	Sn, 100.00	sp ^{0.11}
	LP* Sn(1)	0.14990	Sn, 100.00	p
	BD Sn(2)—O(2)	1.95366	Sn, 3.05 O, 96.95	sp ^{17.18} sp ^{16.08}
	BD Sn(2)—N(3)	1.94877	Sn, 5.34 O, 94.66	sp ^{14.27} sp ^{2.23}
	LP Sn(2)	1.91490	Sn, 100.00	sp ^{0.12}
	LP* Sn(2)	0.14288	Sn, 100.00	p

NBO method. In monomers **4b** and **5b** the central metal atoms are weakly hybridized. For instance, contributions of the M atoms to the NBOs BD M—O and BD M—N mainly involve only p-orbitals with sp^{11.56—14.78} hybridizations (Table 5). The lone electron pairs of the metal atoms (LP M) have strong s-character with sp^{0.16—0.17} hybridizations. Vacant orbitals LP* M with populations of 0.23—0.27 are represented exclusively by the metal p_z-AOs.

Generally, the NBO shape of the metal atoms in dimers **4c** and **5c** are similar to those of the metal atoms in monomers **4b** and **5b**. The metal atoms in **4c** and **5c** are even weaker hybridized than in the monomers (their hybridization in the orbitals BD M—O and BD M—N is sp^{17.18—24.34}). The s-character of the lone electron pairs LP M with the hybridization sp^{0.12} also increases. The LP* M orbital populations decrease to 0.14—0.20.

The M—O and M—N valence bonds in both monomers and dimers have pronounced ionic character. The BD M—O and BD M—N orbitals calculated using the NBO program are strongly polarized toward the O and N atoms. The electron density localization on the metal atoms in molecules **4b** and **5b** is 9.70—13.52%. In dimers **4c** and **5c**, the BD M—O and BD M—N orbitals are even stronger polarized compared to monomers **4b** and **5b**, namely, the electron density localization on the metal atoms is only 3.05—8.22%.

Nonvalent interactions in monomers **4b** and **5b** and in dimers **4c** and **5c** were analyzed in terms of the second-order perturbation theory with the Fock matrix constructed in the NBO basis set.²⁶ A decrease in the energy of the system due to electron density delocalization $\sigma_i \rightarrow \sigma_j^*$ is described as follows:

$$\Delta E_{i \rightarrow j}^{(2)} = -2 \frac{\langle \sigma_i | \hat{F} | \sigma_j^* \rangle^2}{\varepsilon_{j^*} - \varepsilon_i},$$

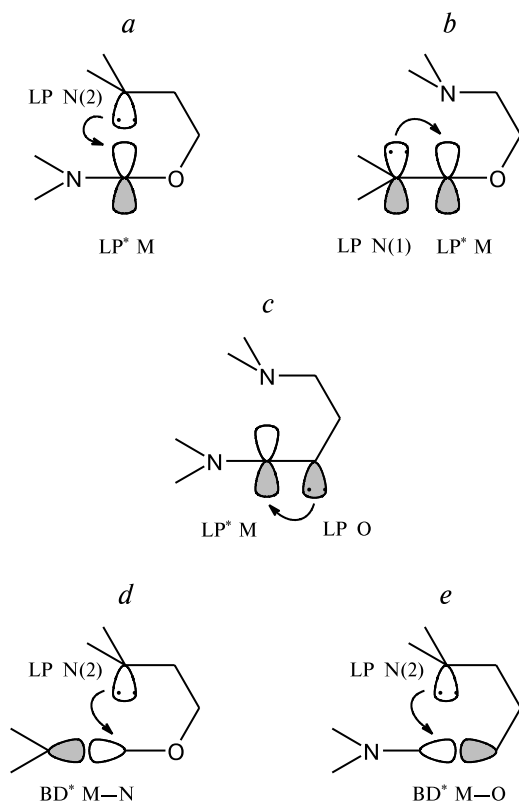
where \hat{F} is the effective orbital Hamiltonian (here, the Kohn—Sham operator), σ_i and σ_j^* are the NBOs, and ε_i and ε_{j^*} are the corresponding NBO energies.

The strongest nonvalent interactions involving metal atoms in monomers **4b** and **5b** correspond to electron density donation from the lone electron pairs of nitrogens in the NMe₂ groups to the vacant p_z-orbital, LP N(2) → LP* M (Scheme 1, **a**; Table 6).

The vacant p_z-orbitals of the metal atoms, LP* M, also interact with the lone pairs of covalently bound nitrogen and oxygen atoms, LP N(1) → LP* M and LP O → LP* M (see Scheme 1, **b** and **c**). Large overlap of the LEP of the nitrogen atoms with the metal p_z-AOs in molecules **4b** and **5b** corresponds to planar arrangement of substituents at the N(1) atoms (see above).

We also found a rather strong interaction between the LEP of the nitrogen atoms in the NMe₂ groups and the

Scheme 1



BD* M—N(1) and BD* M—O(1) antibonding orbitals (see Scheme 1, **d** and **e**). This can be a reason for elongation of the M—N(1) and M—O(1) valence bonds by 0.05 Å upon the formation of M←NMe₂ coordination bonds (transitions **4a** → **4b** and **5a** → **5b**).

In performing NBO analysis of dimers **4c** and **5c** both molecules were treated as two monomer subunits bound through donor-acceptor rather than covalent interactions that were described in terms of second-order perturbation theory $\Delta E_{i \rightarrow j}^{(2)}$.

The main nonvalent interactions within subunits in dimers **4c** and **5c** are of the same nature as the nonvalent interactions in monomers **4b** and **5b**. The highest interaction energies correspond to electron density donation from the NMe₂ groups to the metal atoms, namely, LP N(2) → LP* M(1) and LP N(4) → LP* M(2) (see Table 6). The energies of the interaction between the LEP of nitrogen atoms in the N(SiMe₃)₂ groups and vacant metal p_z-AOs, LP N(1) → LP* M(1), and LP N(3) → LP* M(2), are also high.

The strongest interactions between subunits in dimer **4c** correspond to the Ge←O coordination bonds. Noteworthy is that both electron pairs of the O(1) and O(2) atoms are involved in the formation of coordination contacts Ge(2)←O(1) and Ge(1)←O(2): LP(1) O(1) → LP* Ge(2), LP(2) O(1) → LP* Ge(2) and

Table 6. Most important nonvalent interactions of the atoms M in molecules **4b,c** and **5b,c** in terms of the second-order perturbation theory $\Delta E_{i \rightarrow j}^{(2)}$

Molecule	Donor	→	Acceptor	$\Delta E_{i \rightarrow j}^{(2)}$ kcal mol ⁻¹
4b	LP N(2)	→	LP* Ge(1)	39.5
	LP N(1)	→	LP* Ge(1)	11.6
	LP N(2)	→	BD* Ge(1)—O(1)	6.7
	LP O(1)	→	LP* Ge(1)	6.1
	LP N(2)	→	BD* Ge(1)—N(1)	4.0
5b	LP N(2)	→	LP* Sn(1)	28.9
	LP N(1)	→	LP* Sn(1)	10.2
	LP N(2)	→	BD* Sn(1)—O(1)	5.5
	LP O(1)	→	LP* Sn(1)	3.7
	LP N(2)	→	BD* Sn(1)—N(1)	3.4
4c	LP N(2)	→	LP* Ge(1)	16.5
	LP N(1)	→	LP* Ge(1)	10.8
	LP N(2)	→	BD* Ge(1)—O(1)	4.4
	LP(1) O(1)	→	LP* Ge(2)	17.0
	LP(2) O(1)	→	LP* Ge(2)	7.6
s1 → s2*	LP(1) O(1)	→	LP* Ge(2)	17.0
	LP(2) O(1)	→	LP* Ge(2)	7.6
s2 → s1*	LP(1) O(2)	→	LP* Ge(1)	12.4
	LP(2) O(2)	→	LP* Ge(1)	6.4
s2	LP N(4)	→	LP* Ge(2)	15.1
	LP N(3)	→	LP* Ge(2)	11.2
	LP N(4)	→	BD* Ge(2)—O(2)	2.9
5c	LP N(1)	→	LP* Sn(1)	5.9
	LP N(2)	→	LP* Sn(1)	5.4
	LP N(2)	→	BD* Sn(1)—O(1)	4.3
	LP(1) O(1)	→	LP* Sn(2)	16.2
	LP* Sn(1)	→	LP* Sn(2)	13.3
s1 → s2*	LP(1) O(2)	→	LP* Sn(1)	15.5
	LP* Sn(2)	→	BD* Sn(1)—O(1)	9.1
s2 → s1*	LP(1) O(2)	→	LP* Sn(1)	15.5
	LP* Sn(2)	→	BD* Sn(1)—O(1)	9.1
	LP(1) O(2)	→	LP* Sn(2)	4.8
s2	LP N(3)	→	LP* Sn(2)	4.8
	LP N(4)	→	LP* Sn(2)	4.6
	LP N(4)	→	BD* Sn(2)—O(2)	4.6

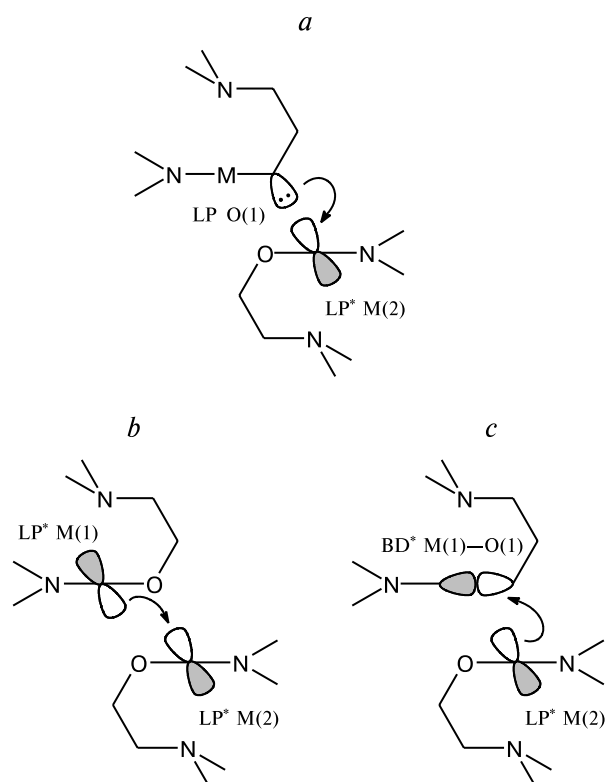
* Electron density donation from one subunit (*s1* or *s2*) to the other subunit.

LP(1) O(2) → LP* Ge(1), LP(2) O(2) → LP* Ge(1) (Scheme 2, **a**). It should also be noted that the interactions between subunits LP O → LP* Ge are comparable in magnitude with the LP N → LP* Ge interaction corresponding to the Ge←NMe₂ coordination bonds within subunits.

In dimer **5c** the types of interactions between two subunits are much different from those found for the germanium compound **4c**. Only one electron pair of the O(1) and O(2) atoms is involved in the formation of the Sn(2)←O(1) and Sn(1)←O(2) coordination bonds, namely, LP O(1) → LP* Sn(2) and LP O(2) → LP* Sn(1) (see Scheme 2, **a**).

The next in energy are the LP* Sn(1) → LP* Sn(2) and LP* Sn(2) → BD* Sn(1)—O(1) orbital interactions (see Scheme 2, **b** and **c**). These interactions involve electron

Scheme 2



density donation to the vacant Sn(2) p_z -AO and to the antibonding orbital of the Sn(1)—O(1) bond. Formally, the LP* Sn(1) and LP* Sn(2) orbitals are vacant and can not act as electron density donors. However, their populations differ from zero (0.15 and 0.14, respectively, see Table 5), which allows such an unusual interaction between the "vacant" orbitals to occur.

The most important difference between the crystal structures of compounds **4** and **5** is that in the crystal the former exists as a monomer while the latter exists as a dimer. The calculated energies of the monomer (**4b** and **5b**) and dimer molecules (**4c** and **5c**) in the gas phase are in agreement with experimental data. For instance, the formation of the tin dimer **5c** from monomer **5b** is an exothermic process with $\Delta E^0 = -11.7$ kcal mol⁻¹ and $\Delta G^0 = -2.1$ kcal mol⁻¹ (see Table 3). The energy of the germanium dimer **4c** is higher than that of monomer **4b** ($\Delta E^0 = 2.5$ kcal mol⁻¹ and $\Delta G^0 = 10.1$ kcal mol⁻¹). The formation of dimers **4c** and **5c** from monomers **4b** and **5b** is affected by steric repulsion between two subunits in the dimer and by the Coulombic and orbital interactions between the subunits.

In dimers **4c** and **5c**, two subunits form four-membered rings M₂O₂. The atoms of these rings are linked by two M—O valence bonds (within subunits) and two M←O coordination bonds (between subunits). Bulky SiMe₃ substituents at the N(1) atoms of amide groups preclude the

formation of the M←O coordination bonds due to steric interaction with methylene groups at the oxygen atoms of the O—CH₂—CH₂—NMe₂ fragments in the oppositely lying subunits in dimers **4c** and **5c**. The Ge—O and Ge—N bonds are ~0.2 Å shorter than the Sn—O and Sn—N bonds, respectively. Thus, the distance from bulky SiMe₃ substituents and methylene groups in the germanium-containing dimer **4c** is shorter than in the tin compound **5c**. Hence, in the former case steric factors produce greater hindrances to dimerization than in the latter case.

The calculated Hirshfeld atomic charge of tin in monomer **5b** is +0.35 (*cf.* +0.26 for the Ge atom in **4b**). Therefore, the Coulombic interaction between the M and O atoms in the M₂O₂ ring in dimer **5c** must be stronger than in dimer **4c**.

The orbital interactions between two subunits in dimers **4c** and **5c** can be analyzed in terms of the second-order perturbation theory $\Delta E_{i \rightarrow j}^{(2)}$ in the NBO basis set. The sum of the $\Delta E_{i \rightarrow j}^{(2)}$ energies corresponding to the interactions between subunits is 232.8 kcal mol⁻¹ for dimer **5c** (the $\Delta E_{i \rightarrow j}^{(2)}$ energies lower than 0.1 kcal mol⁻¹ were ignored) and only 183.4 kcal mol⁻¹ for **4c**. Compared to dimer **4c**, the higher energy of the orbital interactions between subunits in dimer **5c** to a greater extent favors a decrease in its energy relative to the monomer energy.

As a result, the formation of dimer **5c** is favored by both the Coulombic and orbital interactions and the lesser hindrances produced by steric repulsion compared to the formation of dimer **4c**.

* * *

Thus, our DFT and NBO study of the molecular and electronic structure of two stable organic derivatives of divalent germanium and tin, [(Me₃Si)₂N—M—OCH₂CH₂NMe₂]_n (M = Ge (**4**), $n = 1$; M = Sn (**5**), $n = 2$), and their isomers with broken intramolecular coordination bonds M←N showed that the computational method employed correctly reproduces the structural type, main geometric parameters, and energy characteristics of these molecules. Considerable differences between the calculated and experimental interatomic distances were observed only for the M←NMe₂ and M←O coordination bond lengths, which is probably due to the crystal packing effects ignored in the calculations. The formation of the M←NMe₂ coordination bonds ($\Delta E^0 = -5.3$ and -8.6 kcal mol⁻¹ for M = Ge and Sn, respectively) is the main factor responsible for stabilization of these molecules. According to NBO analysis, the metal atoms in molecules **4** and **5** are weakly hybridized. The lone electron pairs of the metal atoms have strong s-character, while the "vacant" orbitals LP* M represented exclusively by the metal np_z -AOs. The M—O and M—N covalent bonds are strongly polarized toward electrone-

gative atoms. The formation of the $M \leftarrow NMe_2$ coordination bonds in molecules **4b**, **5b** and **4c**, **5c** involves electron density donation from the LEP of the nitrogen atoms (LP N) to the vacant orbital of the M atoms ($LP^* M$). In dimers **4c** and **5c** the strongest orbital interaction between subunits is due to electron density donation from the LEP of the oxygen atoms (LP O) to the vacant orbitals of the M atoms ($LP^* M$).

According to calculations, dimerization of **5b** in the gas phase is thermodynamically favorable ($\Delta G^0 = -2.1 \text{ kcal mol}^{-1}$), which is in excellent agreement with experimental data; for **4b**, the process is thermally forbidden ($\Delta G^0 = 10.1 \text{ kcal mol}^{-1}$). The higher relative stability of dimer **5c** compared to dimer **4c** is due to stronger Coulombic and orbital interactions and to lesser steric hindrances produced by repulsion between subunits.

References

1. M. Weidenbruch, *J. Organomet. Chem.*, 2002, **646**, 39.
2. N. Tokitoh and R. Okazaki, *Coord. Chem. Rev.*, 2000, **210**, 251.
3. M. Weidenbruch, *Eur. J. Inorg. Chem.*, 1999, 373.
4. P. P. Power, *J. Chem. Soc., Dalton Trans.*, 1998, 2939.
5. M. Driess and H. Grützmacher, *Angew. Chem., Int. Ed. Engl.*, 1996, **35**, 828.
6. N. N. Zemlyanskii, I. V. Borisova, M. S. Nechaev, V. N. Khrustalev, V. V. Lunin, M. Yu. Antipin, and Yu. A. Ustynyuk, *Izv. Akad. Nauk. Ser. Khim.*, 2004, 939 [*Russ. Chem. Bull., Int. Ed.*, 2004, **53**, 980].
7. O. Köhl, *Coord. Chem. Rev.*, 2004, **248**, 411.
8. R. Okazaki and R. West, *Adv. Organomet. Chem.*, 1996, **39**, 232.
9. N. N. Zemlyanskii, I. V. Borisova, V. N. Khrustalev, Yu. A. Ustynyuk, M. S. Nechaev, V. V. Lunin, J. Barrau, and G. Rima, *Organometallics*, 2003, **22**, 1675.
10. N. N. Zemlyanskii, I. V. Borisova, V. N. Khrustalev, M. Yu. Antipin, Yu. A. Ustynyuk, M. S. Nechaev, and V. V. Lunin, *Organometallics*, 2003, **22**, 5441.
11. V. N. Khrustalev, I. A. Portnyagin, N. N. Zemlyanskii, I. V. Borisova, Yu. A. Ustynyuk, and M. Yu. Antipin, *J. Organomet. Chem.*, 2005, **690**, 1056.
12. V. N. Khrustalev, I. A. Portnyagin, N. N. Zemlyanskii, I. V. Borisova, M. S. Nechaev, Yu. A. Ustynyuk, M. Yu. Antipin, and V. V. Lunin, *J. Organomet. Chem.*, 2005, **690**, 1172.
13. J. P. Perdew, K. Burke, and M. Ernzerhof, *Phys. Rev. Lett.*, 1996, **77**, 3865.
14. M. Ernzerhof and G. E. J. Scuseria, *Chem. Phys.*, 1999, **110**, 5029.
15. C. Adamo and V. J. Barone, *Chem. Phys.*, 1999, **110**, 6158.
16. D. N. Laikov, PhD Thesis, M. V. Lomonosov Moscow State University, Moscow, 2000 (in Russian).
17. W. J. Stevens, H. Basch, and M. J. Krauss, *Chem. Phys.*, 1984, **81**, 6026.
18. W. J. Stevens, M. Krauss, H. Basch, and P. G. Jasien, *Can. J. Chem.*, 1992, 612.
19. T. R. Cundari and W. J. Stevens, *Chem. Phys.*, 1993, **98**, 5555.
20. F. L. Hirshfeld, *Theoret. Chim. Acta. (Berl.)*, 1977, **44**, 129.
21. D. N. Laikov, *Chem. Phys. Lett.*, 1997, **281**, 151.
22. I. V. Borisova, M. S. Nechaev, V. N. Khrustalev, N. N. Zemlyanskii, and Yu. A. Ustynyuk, *Izv. Akad. Nauk. Ser. Khim.*, 2002, 665 [*Russ. Chem. Bull., Int. Ed.*, 2002, **51**, 721].
23. J. P. Foster and F. Weinhold, *J. Am. Chem. Soc.*, 1980, **102**, 7211.
24. A. E. Reed and F. Weinhold, *J. Chem. Phys.*, 1983, **78**, 4066.
25. A. E. Reed, R. B. Weinstock, and F. Weinhold, *J. Chem. Phys.*, 1985, **83**, 735.
26. A. E. Reed, L. A. Curtiss, and F. Weinhold, *Chem. Rev.*, 1988, **88**, 849.
27. E. D. Glendening, J. K. Badenhoop, A. E. Reed, J. E. Carpenter, and F. Weinhold, *NBO 4.M*, Theoretical Chemistry Institute, University of Wisconsin, Madison (WI), 1999.
28. M. W. Schmidt, K. K. Baldridge, J. A. Boatz, S. T. Elbert, M. S. Gordon, J. H. Jensen, S. Koseki, N. Matsunaga, K. A. Nguyen, S. Su, T. L. Windus, M. Dupuis, and J. A. Montgomery, *J. Comput. Chem.*, 1993, **14**, 1347.

Received November 19, 2004